American Mineralogist, Volume 60, pages 785–797, 1975

Mineralogical Zoning in a Scapolite-Bearing Skarn Body on San Gorgonio Mountain, California

KENNETH SHAY[1]

Department of Geology, University of California, Los Angeles, California 90024

Abstract

Concentrically zoned skarns on Mt. San Gorgonio have been studied in detail from the point of view of field and petrographic relations. The skarns are mineralized blocks of marble of the Precambrian San Gorgonio Igneous-Metamorphic Complex, which are within the contact zone between the Complex and the Middle Jurassic Cactus Quartz Monzonite. They consist of cores of calcite-forsterite-diopside marble, surrounded by concentric zones of diopside, actinolite + epidote + calcite + quartz, epidote + garnet + calcite + quartz, and scapolite + calcite + quartz. The genesis of the skarns involved three steps. (1) Regional metamorphism formed tremolite and forsterite from calcite, dolomite, and quartz. (2) The intrusion of the quartz monzonite stabilized diopside + forsterite relative to tremolite + calcite. Reaction between quartz monzonite and marble resulted in the formation of a zone of diopside + wollastonite and a zone of sodic scapolite, by the diffusion of Ca, Mg, and Si across the original contact. Components rejected from this zone formed ferroan diopside in the scapolite zone and in the quartz monzonite, and altered the scapolite to a more calcic form. This process involved a net volume loss of 56.6 percent. (3) Infiltration of fluids, possibly of magmatic origin, formed epidote and garnet from scapolite, and actinolite from diopside.

Introduction

This paper describes the geology and chronicles the geological history of a small group of skarns on Mt. San Gorgonio. Combining textural, mineralogic, chemical, and field data from the skarns with field and petrographic data from a similar area to the south and with published laboratory results, a model for the formation of the skarns is proposed. The model is consistent with the principle of local equilibrium (Thompson, 1959), which has been shown to be a valid assumption in other studies of metasomatism (*e.g.*, Vidale, 1969; Joesten, 1974).

The area studied, hereafter called East Ridge, is at an elevation of 10,500 ft. on the eastern ridge of San Gorgonio Mountain (elevation 11,502 ft.), which is the highest peak in the east-west trending San Bernardino Mountains of southern California (Fig. 1). The San Andreas fault zone defines, and probably formed, the southern scarp which separates the San Bernardinos from the San Jacinto Mountains to the south and the San Gabriel Mountains to the west (Allen, 1957). San Gorgonio Mountain and the surrounding peaks represent a complex of Precambrian metamorphic rocks and Mesozoic intrusives (Vaughn, 1922).

There are relatively few published studies and unpublished theses on the geology of the San Bernardinos; Vaughn (1922) studied the entire range and Baird *et al* (1974) have recently discussed its regional structure. For additional information on the region immediately surrounding East Ridge, the reader is referred to Allen (1957) and Dibblee (1964).

Method of Study

The geology of East Ridge was mapped between May and November, 1973, using a Brunton compass and tape measure, on a 1:240 base map with 5-foot contours mapped in the same fashion (Fig. 2). A total of 120 samples were collected; from these, 70 thin sections, 11 polished sections, and 12 thick sections were prepared, and 60 different whole rock and mineral concentrate powders were ground for XRF and XRD studies.

Seventy different mineral grains were analyzed (Table 1) employing an ARL-EMX microprobe. Standards comparable in composition to the unknowns were not generally available; the standards used are

[1] Current address: Department of Geological Sciences, Harvard University, Cambridge, Massachusetts 02138.

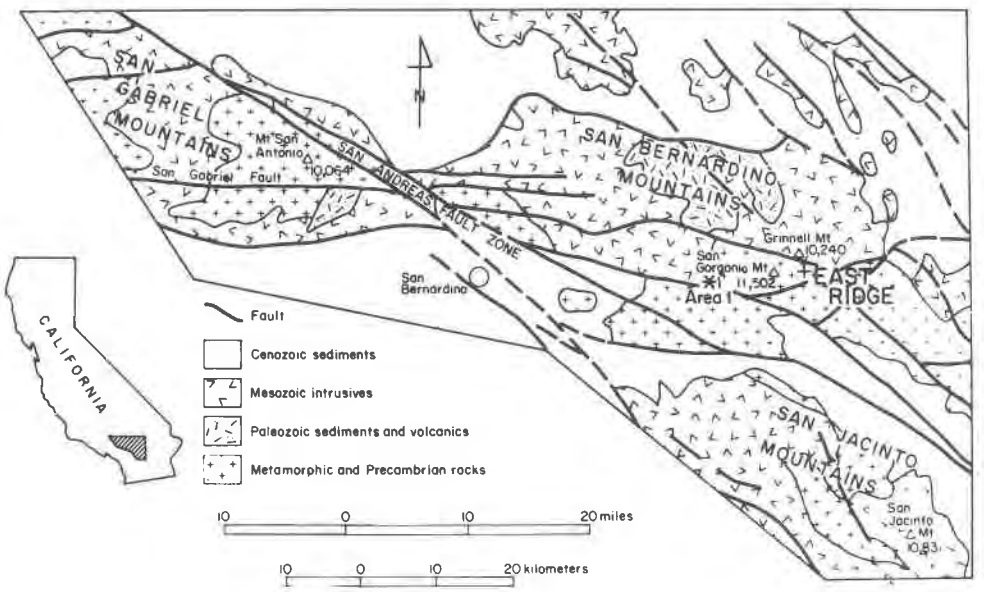

FIG. 1. Index map.

listed in Table 2. Data were reduced using the methods of Bence and Albee (1968) and Albee and Ray (1970).

The XRF whole-rock analyses (Table 3) were done on a Phillips X-ray fluorescence apparatus, using U.S.G.S. Granite G-2, ZGI Granite GM and Basalt BM, and an analyzed limestone as standards.

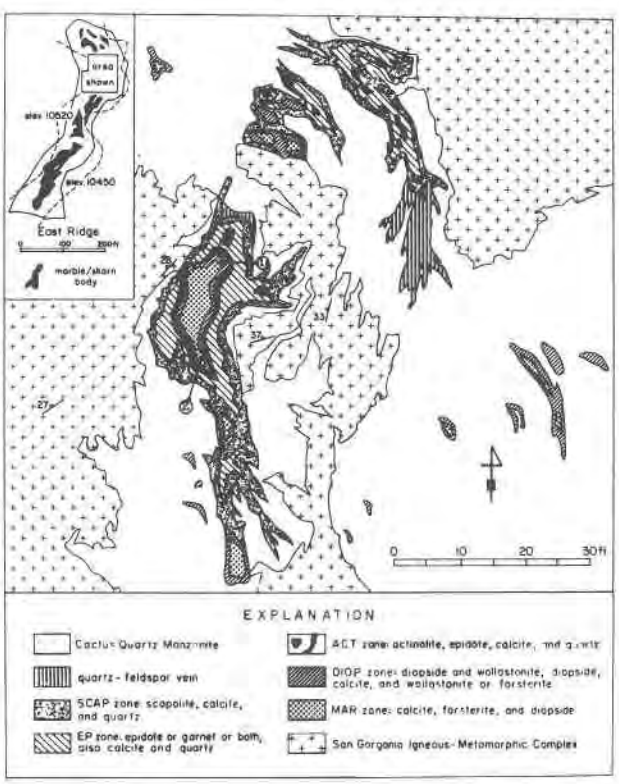

FIG. 2. Geologic map of the northern part of East Ridge (index at upper left). ① shows the sample traverse for Suite 1; ② for Suite 2.

Geology of East Ridge

East Ridge lies within a zone of intrusion and assimilation between the Precambrian San Gorgonio Igneous-Metamorphic Complex and the Middle Jurassic Cactus Quartz Monzonite (Fig. 2). The Complex apparently has not been deformed by this intrusion, as foliation is consistent throughout the contact zone, and faults, with maximum offset 10 m, postdate the intrusion.

Cactus Quartz Monzonite

This coarse-grained (1-4 mm) granitic intrusive, originally called the Cactus Granite by Vaughn (1922) but renamed the Cactus Quartz Monzonite by Guillou (1953), contains about 30 percent each of quartz, oligoclase (An_{26}), and K-feldspar, and 10 percent biotite with accessory apatite, tourmaline, sphene, zircon, magnetite, and allanite (in biotite). Hornblende is rare and where present, of glomeroporphyritic habit. Hollenbaugh (1968) considers the Cactus to be comagmatic with a pegmatite that Hewett and Glass (1953) dated as Middle Jurassic. This is in agreement with more recent K-Ar ages (Armstrong and Suppe, 1973).

San Gorgonio Igneous-Metamorphic Complex

This Precambrian complex, named by Allen (1957), includes migmatite and gneiss (microcline-

TABLE 1. Microprobe Analyses in Weight Percents

Sample No.*	AC05902	AC12402	AC12409	AC12410	AC12503	AC12504	DI01701	DI01704	DI06602A	DI06602B	DI06603A	DI06603C	DI06604	DI06604A
Location**	ACT	ACT	ACT	ACT	ACT	ACT	SCAP	SCAP	DIOP	DIOP	DIOP	DIOP	DIOP	DIOP
SiO_2	51.5	52.7	52.4	55.8	51.4	53.6	51.4	52.0	54.2	54.0	54.0	54.0	53.6	53.5
Al_2O_3	3.9	2.3	1.5	.8	1.4	.9	.7	.4	.4	.3	.1	.4	.4	.7
CaO	12.4	12.8	12.7	13.1	12.6	12.7	24.3	24.4	25.2	25.5	25.6	25.5	25.0	25.7
Na_2O	0.0	.2	.3	tr	.5	.4	.2	.2	.1	tr	.1	tr	.1	tr
Fe as FeO	13.2	12.3	12.8	6.9	14.7	13.3	11.2	10.8	2.1	2.0	2.1	1.5	2.9	2.5
MgO	13.5	15.8	16.0	19.7	15.5	16.9	11.2	11.4	17.5	17.6	17.4	17.6	17.4	17.3
TiO_2	.2	.2	.1	0.0	tr	0.0	tr	tr	tr	tr	tr	tr	tr	tr
MnO	.8	.5	.6	.5	.6	.5	.7	.6	.3	.2	.2	.3	.3	.3
Cl	na	na	na	na	na	na	na	na	na	na	na	na	na	na
H_2O	3.4	3.2	3.6	3.2	3.2	1.7	0	0	0	0	0	0	0	0
Total	100.0	100.0	100.0	100.0	100.0	100.0	99.7	99.8	99.7	99.6	99.5	99.4	99.7	100.0

Sample No.*	DI06604B	DI06605A	DI07901	DI07902A	DI07902B	DI07903	DI12301E	DI12301F	DI12303A	DI12304	DI12305A	DI12305B	DI12305C	DI12306
Location**	DIOP	DIOP	m.v.	m.v.	m.v.	m.v.	EP	EP	EP	ACT	ACT	ACT	ACT	ACT
SiO_2	53.3	53.7	52.5	52.0	52.8	52.8	52.1	52.0	51.7	51.5	51.6	51.3	51.9	51.8
Al_2O_3	.3	.8	.5	.6	.6	.6	.4	.5	.5	.4	.6	.5	.6	.6
CaO	25.2	25.2	24.7	24.5	24.9	24.8	24.4	24.4	24.6	24.3	24.5	24.5	24.5	25.1
Na_2O	.1	.1	.2	.3	.2	.2	.2	.2	.2	.3	.2	.2	.2	.1
Fe as FeO	3.1	2.9	9.0	12.4	9.0	11.4	11.7	10.4	10.6	12.0	11.7	12.3	11.3	9.8
MgO	18.1	16.8	12.5	10.8	12.4	9.6	11.2	10.8	10.9	9.9	10.5	10.1	10.5	11.2
TiO_2	tr	tr	tr	tr	tr	tr	tr	tr	tr	tr	tr	tr	tr	tr
MnO	.3	.3	.3	.2	.2	.5	1.0	1.1	1.2	1.2	1.2	1.1	1.2	.8
Cl	na	na	na	na	na	na	na	na	na	na	na	na	na	na
H_2O	0	0	0	0	0	0	0	0	0	0	0	0	0	0
Total	100.4	99.7	99.7	100.9	100.0	99.8	101.0	99.5	99.8	99.6	100.2	100.1	100.2	99.4

Sample No.*	DI12408	DI12410	DI126B02	EP01705A	EP12202	EP12203	EP12303A	EP12401	EP12402	EP12402A	EP12403	EP12404	EP12409	EP12501
Location**	ACT	ACT	EP	EP	SCAP	SCAP	EP	EP	EP	EP	EP	EP	EP	ACT
SiO_2	54.5	54.5	52.6	36.9	37.2	37.2	37.4	36.5	36.6	36.9	37.4	37.1	36.9	36.8
Al_2O_3	.2	.3	.6	22.9	23.2	23.3	22.1	22.2	22.9	22.7	23.4	23.0	22.5	23.2
CaO	25.6	25.4	24.3	23.1	23.0	23.0	23.7	23.1	23.2	23.3	23.5	23.2	23.2	23.3
Na_2O	tr	tr	na	tr	0.0	0.0	tr	tr	tr	tr	tr	tr	tr	tr
Fe as FeO	1.2	1.5	11.8	12.8	12.2	12.2	13.0	12.2	12.5	12.4	12.1	12.4	12.9	12.1
MgO	17.7	17.8	9.6	0.0	0.0	0.0	0.0	0.0	.2	0.0	0.0	.2	0.0	0.0
TiO_2	tr	tr	na	.1	0.0	0.0	.1	0.0	0.0	.2	0.0	tr	.1	.3
MnO	tr	tr	1.3	.2	.2	.2	.2	.1	.1	.2	.1	.1	.3	.2
Cl	na	na	na	na	na	na	na	na	na	na	na	na	na	na
H_2O	0	0	0	3.9	4.1	4.0	3.5	4.3	4.5	4.3	3.4	4.0	4.0	4.0
Total	99.3	99.5	100.2	99.9	100.0	100.0	100.0	100.0	100.0	100.0	100.0	100.0	99.9	99.9

Sample No.*	EP12502	EP12601	EP126B02	FO06601	FO06602	GA00003	GA00004	GA07005	GA12301A	GA12302	GA12306	SC01502	SC01701	SC01701A
Location**	ACT	EPe	EPe	DIOP	DIOP	EP	EP	EP	EP	EP	EP	SCAP	SCAP	SCAP
SiO_2	36.8	36.5	36.8	39.7	40.0	37.9	37.7	37.7	36.8	37.8	37.9	45.4	46.2	56.3
Al_2O_3	23.4	23.4	23.6	.1	.1	14.8	14.8	14.2	10.7	11.1	13.9	26.2	24.8	24.9
CaO	23.3	23.1	23.0	.1	.1	34.7	34.7	34.1	32.3	33.4	34.7	17.3	17.3	9.1
Na_2O	tr	0.0	0.0	0.0	0.0	tr	tr	tr	tr	tr	tr	3.9	3.6	6.4
Fe as FeO	12.4	12.8	12.2	7.9	7.7	11.0	11.4	13.1	16.5	15.7	11.7	.2	.1	.1
MgO	0.0	0.0	tr	51.7	51.5	tr	tr	0.0	tr	tr	.1	0.0	0.0	0.0
TiO_2	.1	0.0	0.0	tr	tr	.3	.3	tr	.8	.1	.7	0.0	0.0	0.0
MnO	.1	.1	.2	.2	.4	.7	.9	.5	2.0	1.3	.9	tr	tr	tr
Cl	na	na	na	na	na	na	na	na	na	na	na	tr	tr	tr
H_2O	3.8	4.0	4.2	0	0	0	0	0	0	0	0	0	0	0
Total	100.0	100.0	100.0	99.7	99.7	99.4	99.8	99.7	99.2	99.5	99.8	93.0***	92.0***	96.7***

Sample No.*	SC01701B	SC01701E	SC01702A	SC01702B	SC01706B	SC01701	SC07801	SC07901	SC07903	SC12201	SC12204	SC12205	WL07903	WL07904
Location**	SCAP	SCAP	SCAP	SCAP	SCAP	SCAP	m.v.	m.v.	m.v.	SCAP	SCAP	SCAP	DIOP	DIOP
SiO_2	56.5	57.1	46.1	45.9	57.2	45.0	45.7	46.3	46.3	45.9	45.5	46.7	51.1	51.1
Al_2O_3	24.7	24.8	25.5	25.4	24.8	26.0	25.6	26.1	26.3	27.5	26.2	25.5	.1	.1
CaO	8.7	8.5	17.5	17.9	8.3	17.5	16.8	16.7	17.0	15.4	17.4	17.1	48.2	48.3
Na_2O	6.7	6.6	3.8	3.8	6.6	3.7	3.5	3.3	3.3	3.6	3.6	3.8	tr	tr
Fe as FeO	.1	.1	.1	.1	.1	.1	.1	.2	.2	.1	.1	.1	.1	.1
MgO	0.0	0.0	0.0	0.0	0.0	0.0	0.0	tr	0.0	0.0	0.0	0.0	0.0	0.0
TiO_2	0.0	tr	tr	tr	0.0	0.0	tr	0.0	0.0	0.0	0.0	0.0	0.0	0.0
MnO	0.0	tr	0.0	tr	tr	tr	tr	tr	tr	tr	tr	tr	.1	.1
Cl	tr	tr	tr	tr	tr	tr	.4	.3	.4	tr	tr	tr	na	na
H_2O	0	0	0	0	0	0	0	0	0	0	0	0	0	0
Total	96.7***	97.0***	93.1***	93.1***	96.9***	92.3***	92.2***	92.9***	93.5***	92.6***	92.9***	93.2***	99.6	99.7

*First two letters designate mineral: AC = actinolite; DI = diopside; EP = epidote; FO = forsterite; GA = garnet; SC = scapolite; WL = wollastonite.
**Refers to mineralized zone. m.v. = diopside-scapolite veins in MAR zone.
***No analysis for CO_2.

TABLE 2. Standards Used in Microprobe Analyses

Element	Standard	Element	Standard
Al	pyrope garnet	Mn	spessartine garnet
Ca	wollastonite	Na	albite
Cl	halite	Si	pyrope garnet
Fe	magnetite	Ti	synthetic rutile
Mg	pyrope garnet		

quartz, biotite-microcline-quartz, biotite-amphibole, magnetite-biotite-amphibole), schist (muscovite-biotite-quartz, biotite-microcline-quartz), quartzite, and marble. Allen places the assemblages in the kyanite-staurolite subfacies of Turner's (1948) amphibolite facies. Silver (1971) reports a zircon age of at least 1750 ± 15 m.y. for a granite which intrudes a gneiss of this complex, thereby confirming the Precambrian age suggested by Dibblee (1964).

Marble and Skarn

The marble bodies at East Ridge and the 1- to 250-cm wide bands of skarn surrounding them are here discussed together. A total of eleven individual bodies with nearly complete mineralogic zonation (described below) are present. The maximum exposed thickness is 8.9 m (27 ft), and as that widest part is bounded above by gneiss and below by quartzite and schist, this is taken to be the maximum thickness. Thinner bodies have a thinner marble core or may even lack a carbonate core, occurring simply as large pods of concentric garnet-, epidote-, actinolite-, diopside-, and scapolite-rich bands. Along strike, the length of exposure of the skarns is approximately 150 m (460 ft).

The bands of skarn surrounding the marble cores (the MAR zone) have been designated as the DIOP, ACT, EP, and SCAP zones. Two suites of samples from the zones were collected, as shown in Figure 2. Calcite is present everywhere except in most of the DIOP zone; and with the exception of the MAR and DIOP zones which contain accessory ilmenite, quartz and sphene are ubiquitous (Fig. 3; Table 4).

MAR Zone. At East Ridge, much of the exposed marble has been extensively mineralized and altered; consequently many original features, in particular the originial composition, are unclear. However, the southernmost skarn body at East Ridge contains a marble core which bears an extremely close lithologic and stratigraphic relationship to rock of Area 1 (Fig. 1), an interbedded schist-marble-gneiss sequence which has not been intruded so pervasively. The thickness, grain size, bulk composition, and stratigraphic position of the two marbles are virtually identical. It is fair to assume that originally all of the East Ridge marble was nearly identical to the Area 1 marble, and this assumption will be used to augment and interpret the data from East Ridge. The effects of intrusion of quartz monzonite at Area 1 are discussed below.

The East Ridge marble, the MAR zone, is 35-40%

TABLE 3. Partial XRF Analyses, Weight Percents

Sample No.	73-58	73-85	73-59	73-19	73-66	73-71	73-131	73-125	73-124	73-132	73-122	73-129	73-53q	73-75	73-14
Location†	MAR	MAR	MAR	DIOP	DIOP	DIOP	ACT	ACT	EP	EP g	SCAP	SCAP	q	.1	.2
SiO_2	10.82	11.45	15.62	51.25	50.27	51.77	51.45	55.85	51.41	53.02	50.02	52.38	86.78	68.89	69.92
Al_2O_3	.28	.16	1.64	1.42	1.84	1.71	8.53	4.87	13.73	14.58	25.25	24.28	6.06	14.39	16.03
CaO	34.85	34.02	38.06	23.86	25.77	24.80	22.91	21.89	19.96	12.40	14.86	10.66	3.69	4.96	1.55
Na_2O	1.32	.48	.42	.12	.18	.16	.01	.00	.00	.00	3.05	5.08	.40	2.03	2.90
Fe as FeO	1.10	.37	2.41	4.35	4.49	4.38	9.45	9.13	6.57	6.48	2.99	2.48	1.76	2.06	1.40
MgO	14.32	13.75	13.71	16.81	16.99	16.26	5.83	6.88	5.27	3.51	.95	.51	1.15	1.39	.65

Sample No.	73-128	73-134	73-135	73-136	73-138	73-139	73-140	73-141	73-142	73-72	73-144	73-145	73-146	73-147	73-148
Location†	.5	1	1	1	2	2	3	3	4	4	5	6	6	7	7
SiO_2	69.05	69.95	74.84	70.67	69.99	75.93	73.07	75.76	75.70	71.97	76.61	76.10	72.00	77.28	73.88
Al_2O_3	15.54	14.73	13.78	15.33	15.70	13.43	14.44	13.67	13.39	15.84	13.32	13.39	15.07	12.72	13.99
CaO	3.32	2.72	.82	2.88	2.68	.95	1.07	1.05	.93	2.48	1.24	1.12	1.77	.75	1.35
Na_2O	4.46	5.30	2.42	4.07	4.01	2.58	3.07	2.84	2.56	3.75	3.06	2.87	2.11	2.53	2.56
Fe as FeO	3.29	2.99	.86	2.37	2.72	.69	1.24	.73	.75	1.61	.69	.82	.5	.86	1.45
MgO	1.04	.93	.28	.68	.72	.31	.48	.30	.28	.36	.24	.26	.53	.19	.43

Sample No.	73-149	73-150	73-151	73-152	73-153	73-76	73-154	73-155	73-73	73-6	73-32	73-33
Location†	8	8	9	9	10	10	15	16	65	>100	>100	>100
SiO_2	73.26	76.62	73.60	75.71	76.09	76.04	76.23	72.84	74.85	74.00	73.78	73.74
Al_2O_3	14.58	12.71	14.08	13.40	12.73	12.57	13.51	14.70	13.91	14.05	14.23	14.47
CaO	.75	1.35	1.41	.84	.81	1.23	.84	1.51	1.22	1.27	1.89	1.53
Na_2O	3.19	2.68	1.73	3.02	2.93	2.17	3.35	3.29	2.64	3.42	3.21	4.29
Fe as FeO	1.09	.87	.41	.95	1.21	1.81	.93	.91	.67	1.48	1.53	1.49
MgO	.46	.24	.47	.27	.56	.43	.28	.54	.31	.34	.35	.43

†*Refers to skarn zones, or distance (in feet) into quartz monzonite from contact. "q" is quartz-feldspar veins. Analyst: P.C. Stummer*

forsterite, 55-60% calcite, 5% diopside, and 1% tremolite; the Area 1 marble is 45% forsterite, 45% calcite, and 10% tremolite (see Fig. 3). The olivine in the MAR zone is fine- to medium-grained, anhedral, and has the composition $Fo_{92.5}$, with trace amounts of Mn, Al, Ca, and Ti. The tremolite is fine-grained, colorless, elongate, and rimmed by forsterite and diopside in the MAR zone. The diopside grains are untwinned, equant, fine- to medium-grained, and pale green. Their composition is $Di_{95}Hd_5$; the rims are enriched in Fe.

In all the Area 1 marble outcrops studied, there is a 0.3-1 cm wide weathered-out space between marble and schist (below) or gneiss (above). This may be due to a metasomatically formed reaction zone which has been weathered out. The outcrops are so extensively weathered that no analyses were performed on the Area 1 samples.

In several instances, zoned veins are present within the MAR zone. The centers of such veins are composed of quartz and medium- to extremely coarse-grained scapolite, in approximately equal proportions. The scapolite is milky and euhedral to subhedral, fluoresces orange, is inclusion free, and has the composition $Ca_2NaAl_5Si_7O_{24}\cdot(CaCO_3)_{0.8}\cdot(NaCl)_{0.1}$. Between this assemblage and the host marble is a band of fine to medium-grained, pale green diopside. The grains are equidimensional, generally twinned, and compositionally homogeneous; the average formula is $Di_{60}Hd_{40}$ with trace Al, Mn, Na, and Ti. This pyroxene will henceforth be referred to as "Fe-diopside," to emphasize the difference between it and the more magnesian pyroxene, "Mg-diopside," described two paragraphs above.

DIOP Zone. The DIOP zone is defined by the innermost appearance of a rock of >50 percent Mg-diopside, and contains diopside, wollastonite, calcite, and forsterite. The center of the zone is 90-95 percent diopside and 5-10 percent wollastonite. Near the boundary with the MAR zone 2-5 percent each of wollastonite and calcite, or 2-3 percent each of calcite and forsterite, are present.

The diopside is identical to that present in the MAR zone. The forsterite has been extensively replaced by serpentine and has the same composition as the forsterite present in the MAR zone. The wollastonite is fibrous and fluoresces blue-green. Its composition is very nearly $CaSiO_3$, with 1 wt percent or less each of Al and Fe.

ACT Zone. A sharp boundary exists between the DIOP and ACT zones, defined by the innermost appearance of green to yellow-green actinolite and epidote in lesser amounts. Near the DIOP/ACT boundary, actinolite is by far the prominent mineral in the ACT zone, but generally decreases in amount with increasing epidote, toward the ACT/EP boun-

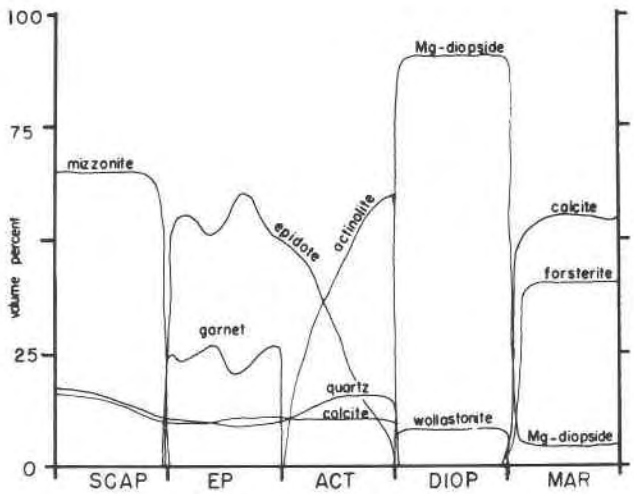

FIG. 3. Mineralogic variation at East Ridge, based on the estimated modes of Suite 1.

TABLE 4. Estimated Modes of Samples From the East Ridge Zones
(*In Volume Percent*)

Zone:	MAR		DIOP	ACT	EP	SCAP
Suite 1:	58	66	19	125	124	122
quartz	--	--	--	15	10	15
calcite	55	5	--	10	10	15
dolomite	--	--	--	--	--	--
Mg-diopside	5	90	90	--	--	--
forsterite	40	3	--	--	--	--
wollastonite	--	--	8	--	--	--
tremolite	1	--	--	--	--	--
mizzonite	--	--	--	--	--	65
epidote	--	--	--	15	55	--
garnet	--	--	--	--	25	--
actinolite	--	--	--	60	--	--
ilmenite	>2	>2	>2	>1	--	--
sphene	--	--	--	--	>2	5
Suite 2:	85	71		131	132(Ep_g)	129
quartz	--	--		20	10	30
calcite	60	4		5	5	15
dolomite	--	--		--	--	--
Mg-diopside	5	90		--	--	--
forsterite	35	--		--	--	--
wollastonite	--	4		--	--	--
tremolite	1	--		--	--	--
mizzonite	--	--		--	--	50
epidote	--	--		35	--	--
garnet	--	--		--	85	--
actinolite	--	--		40	--	--
ilmenite	>2	>2		--	--	--
sphene	--	--		>2	2	5

Samples were taken from centers of zones except for: 66, taken from MAR/DIOP boundary; 71, taken close to that boundary; 125, taken near DIOP/ACT boundary; and 131, taken near ACT/EP boundary.

dary. Quartz plus calcite constitute 25 percent of the zone.

The actinolite is fine- to medium-grained, extensively intergrown with calcite, and is commonly found replacing Mg-diopside. The average composition of the analyzed grains is $Ca_{1.9}Mg_{3.5}Fe_{1.6}Al_{0.5}Si_{7.5}O_{22}(OH)_2$ with trace amounts of Mn, Na, and Ti. The epidote crystals are medium-grained and amoeboid, with inclusions of quartz, calcite, and the ferroan diopside, Fe-diopside. Composition within a single grain may vary, but no systematic zoning was observed. Throughout East Ridge, the average epidote composition is consistently $Ca_2Al_{2.1}Fe_{0.9}Si_3O_{12}(OH)$.

EP Zone. The outermost occurrence of actinolite marks the boundary between the ACT and EP zones. The EP zone can be broken down into three subzones, none of which shows a preference for any particular position within the zone. The least common of these, the EPg, is composed almost entirely of garnet, with 10 percent quartz and calcite. The garnet is extremely coarse-grained, with crystals as large as 2.5 cm. Grains are enriched in Mn in the center and Fe at the rim; the average composition is $Gr_{55}Andr_{45}$, with minor Mn and Ti. Inclusions of Fe-diopside are abundant, as are inclusions of quartz and thin calcite veins.

A second, more prevalent subzone, the EPe, is composed almost exclusively of extremely coarse-grained, euhedral epidote with the same composition as the epidote of the ACT zone. Inclusions of quartz and Fe-diopside are fairly common.

The most common subzone, considered as generally representative of the zone and therefore designated simply as EP, consists of 25-70 percent epidote and 10-60 percent garnet, with 10-20 percent quartz and 10 percent calcite. The garnet and epidote have compositions identical to those of the EPe and EPg subzones, and seem to have formed simultaneously, as seen by intergrowths between the two minerals. The grains tend to be extremely large and anhedral, and contain inclusions and veins like those described. The epidote:garnet ratio increases slightly from north to south.

SCAP Zone. The SCAP zone, as mapped, is bounded on the intrusive side by either the quartz monzonite or by aplitic quartz-feldspar veins and on the EP zone side by the innermost occurrence, other than the MAR zone veins, of scapolite. In fact, however, the SCAP-quartz monzonite contact is not clearly defined, because euhedral, spongiform crystals of scapolite up to 2 cm long surrounding quartz, biotite, oligoclase, K-feldspar, and Fe-diopside are commonly observed in the quartz monzonite. For 1-7 cm beyond this transition zone, the quartz monzonite contains up to 5 percent Fe-diopside. Veins of epidote less than two millimeters across cut across the SCAP zone, running from the quartz monzonite to the EP zone. Similar veins are present at contacts with schist and gneiss all over East Ridge; none are present at Area 1.

Three compositional varieties of scapolite are present at East Ridge. The predominant scapolites of the SCAP zone, and the only ones in the adjacent quartz monzonite, are colorless, euhedral, and up to 4.5 cm in length. The largest crystals are spongiform, consisting of 40 percent inclusions of Fe-diopside, quartz, sphene, and a second scapolite, as well as minerals of the quartz monzonite, as noted. Myrmekitic intergrowths of quartz and veins of calcite are abundant. The host scapolite grains are homogeneous, with composition $Ca_{1.9}Na_{1.1}Al_{4.9}Si_{7.1}O_{24}\cdot(CaCO_3)_{0.9}$. The second type of scapolite is found only as fine-grained, anhedral, polysynthetically-twinned inclusions within grains of the first type. This scapolite has composition $Ca_{1.1}Na_{1.9}Al_{4.1}Si_{7.9}O_{24}\cdot(CaCO_3)_{0.3}$. The third type is the Cl-bearing variety in the MAR zone veins.

In the East Ridge scapolites, the coefficients of the $CaCO_3$ and NaCl ideally should total 1.0, but based on 34 analyses, Shaw (1960) has found a slightly lower value, 0.855. Analyses in which the sum is less than this value could be indicative of variable amounts of K_2CO_3, K_2SO_4, and KOH, for which no analyses were performed. Other possible explanations for the low sums are vaporization by the analyzing beam, natural deviation from the ideal formulae, or poor analyses. The composition of a scapolite can be approximated as a solid solution between meionite, $Ca_3Al_6Si_6O_{24}\cdot CaCO_3$ (Me), and marialite, $Na_3Al_3Si_9O_{24}\cdot NaCl$ (Ma). Intermediate species are named dipyre (Me_{20-50}) and mizzonite (Me_{50-80}), with appropriate prefixes to designate the "ligand molecule," *e.g.*, NaCl (Solodovnikova, 1951). To distinguish the different scapolites of East Ridge, these specific names will be used: dipyre for the sodic variety, mizzonite for the calcic.

Other Features. Mineralized blocks <0.3 m across, of what were originally marble, are present throughout the quartz monzonite surrounding the main skarn bodies. These xenoliths lack scapolite, epidote, and garnet, having instead a zonation from inner marble, like that of the MAR zone, to a zone of Mg-diopside. This is in turn surrounded by a thin

zone of dark-green actinolite (too thin to be shown in Fig. 2) which lacks calcite intergrowths. The smallest of these xenoliths lack marble cores.

The contact sequence at Area 1 was studied for comparison. Here the intrusive is separated from the marble by a band of dipyre (*dr* zone), followed by a zone of Mg-diopside and wollastonite identical to the DIOP zone at East Ridge. The diopside and dipyre occur together over a width of 0.6 cm, and dipyre is present in the quartz-enriched contact between *dr* and quartz monzonite. The widths of the zones vary but are approximately in the ratio *dr*: DIOP = 2:1.

Bulk Rock Composition. Variations in the chemical compositions of the rocks of the two East Ridge suites, and quartz monzonite samples up to 2.13 m (7 ft) from the contact, are shown in Figure 4. Analyses of quartz monzonite collected further than this from the contact are consistent with those from 1 to 2.13 m.

Discussion

In order to discuss the processes which are responsible for the East Ridge zonation, a rough sequence of events leading to the present mineralogic configuration must first be established. Petrographic and

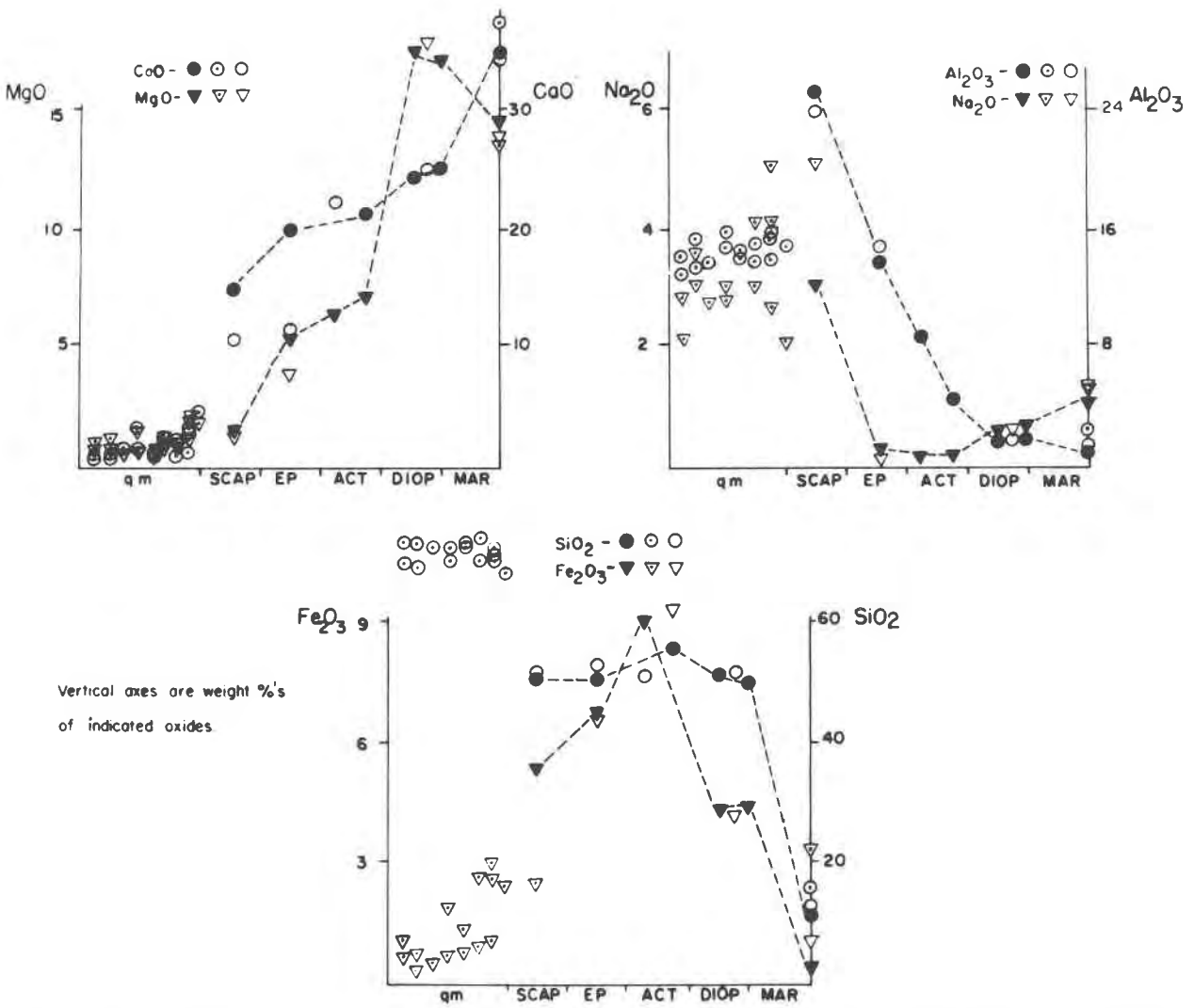

FIG. 4. Bulk chemical analyses of Suites 1 (colored in) and 2, and quartz monzonite up to 7 ft from contact. Dashed lines connect Suite 1 rocks and do not necessarily represent the character of variation between points. Dots within circles represent analyses of rocks of neither Suite 1 nor 2.

field evidence show that there were three different episodes of metamorphism:

Step 1: Regional metamorphism of a calcite-dolomite-quartz marble formed tremolite and forsterite. This is suggested by the similar composition, but different mineralogy, of the Area 1 marble (see Figure 6).

Step 2: The next step, which accompanied the intrusion of the quartz monzonite, was the formation of two mineralogic zones, similar to those seen at Area 1, between the intrusive and the marble. Contemporaneous with the formation of these zones, tremolite + calcite in the marble reacted to form diopside + forsterite + CO_2. Following this, Fe-diopside and then mizzonite were formed in the outer (*dr*) contact zone and in veins in the marble. These minerals are not present at Area 1, indicating that this locality may represent a preliminary state of East Ridge.

Step 3: Epidote, garnet, actinolite, calcite, and quartz formed by reactions between late-stage magmatic fluid and contact minerals.

Step 2

The two initial contact zones of Step 2, the *dr* and the DIOP, formed by diffusion and reaction between the intrusive and country rocks. To better understand the growth of the zones, we must first establish a reference frame to which we can relate the motions of components and zone boundaries. The reader should note that only net relative movements can be deduced in this study, because only the final state, and questionable data on the initial state, are known for the system. Determination of detailed mechanisms of formation (*e.g.*, whether the components diffuse through a crystalline or fluid medium), and values for fluxes and diffusion coefficients of components, require experimental studies.

Although, in principle, movement relative to one reference frame can be related to movement relative to any other, certain reference frames may be more illuminating than others for a given situation. The problem then, is to choose the one best suited to the particular constraints of the system. Brady (1975) has discussed several possibilities, including (1) mean volume reference frame, (2) K^{th}-component reference frame, and (3) inert marker reference frame.

Movement of Components; Original Contact. The mean volume reference frame is most useful for constant volume processes, and so does not lend itself to the problem at East Ridge, because of the volume loss owing to decarbonation reactions. However, the only requirement for the K^{th}-component reference frame is that the flux of some K^{th}-component with respect to that frame is zero. In other words, using this frame is the same as considering one component as motionless, and comparing the net movements of other components relative to it. In discussing such a transfer of components at East Ridge, it is convenient to express the components as oxides, because only the net movement can be deduced, and the oxide form simplifies chemical comparisons between assemblages.

If a K^{th}-component which truly did not move with respect to an inert (non-diffusing) marker frame is present, of if some inert marker like graphite is present (Vidale, 1969), then the location of the original contact is easily deduced. Probably all of the components do move relative to an inert marker frame (Vidale, 1969), so it is conceptually most useful to choose as the K^{th}-component the slowest, or "most nearly motionless" component. Previous workers (*e.g.*, Carmichael, 1969) have argued that this component is $AlO_{3/2}$. Assuming that the $AlO_{3/2}$ reference frame coincides with an inert marker frame, it follows that the original contact is within the border zone lying between the *dr* and DIOP zones, which at East

TABLE 5. Composition of Zones (in Moles/100 cm³)

	MAR	DIOP	"dr"	ACT	EP	SCAP	Avg. Qtz. Monz.
Density (gm/cc)*	2.94	3.24	2.66	3.10	3.58	2.56	2.64
SiO_2	.545	2.714	2.331	2.73	3.057	2.182	3.27
$\frac{1}{2}Al_2O_3$	.013	.117	1.210	.408	.965	1.244	.722
CaO	1.805	1.491	.590	1.289	1.274	.582	.064
$\frac{1}{2}Na_2O$	.085	.019	.590	-	.016	.336	.271
FeO	.029	.196	-	.401	.427	.133	.037
MgO	1.024	1.367	-	.489	.13	.062	.024

*Based on data of Robie and Waldbaum (1968)

Ridge is within the ACT zone. The movements of other components relative to the $AlO_{3/2}$ reference frame have been tabulated (Table 6). These data suggest that there was a total volume loss in the contact zone of 56.5 percent. Figures based on the MgO reference frame have been computed for comparison.

The volume loss due to decarbonation may be estimated by a consideration of the CaO contents of the quartz monzonite and *dr* zone. Specifically, it may be assumed that in the *dr* zone, the CaO concentration (increased by 56.5%) greater than that of the similarly-adjusted quartz monzonite is due to the addition of CaO that was once present as calcite. Using the data in Table 5, the volume loss due to decarbonation in the formation of the *dr* zone is calculated as 19.5 percent.

Driving Forces of Metasomatism. Thompson (1959) and Vidale (1969) discussed movement of components down a gradient of "non-volatile component" (*e.g.*, SiO_2, MgO) activity. Hewitt (1973) has shown that mineralogic banding may be due to a gradient in "volatile" (*e.g.*, H_2O) composition as well. Both mechanisms are possible for East Ridge: there was most certainly some variation in fluid composition between the CO_2-rich fluid of the marble and the H_2O-rich fluid of the magma; and the variation in "non-volatile" composition between the SiO_2- and $AlO_{3/2}$-rich quartz monzonite and the CaO- and MgO-rich marble makes a non-volatile component activity gradient possible. The following discussion demonstrates that both gradients have affected the East Ridge rocks.

In Figure 5a the bulk compositions of the Step 2 zonation, from quartz monzonite to marble, are plotted against molecular CaO, MgO, SiO_2, and $AlO_{3/2}$ content. The plot clearly indicates the increase of a_{SiO_2} from the marble to the *dr* zone, and decrease of a_{CaO} over the same path. It is clear that CaO and SiO_2 have indeed diffused "down" the potential gradients (Fig. 5b,c).

Treating each zone as an open system in thermodynamic equilibrium (Thompson, 1959), it has been shown that for an arbitrary temperature and pressure, the minimum number of "inert components" (those components whose chemical potentials are controlled by the phases—Korzhinsky, 1959) is *n* for an *n*-phase zone. Variation in *n*, and therefore in the number of phases, from one zone to the next may be due to an inert component becoming "mobile" for a zone (see Vidale and Hewitt, 1973).

It is worthwhile to discuss (1) why the assemblages depicted in Figure 5a only approximate but never attain the path along the line calcite-diopside, to the point *Diopside;* and (2) why it is this path that is approached. The second point is fairly obvious: to get between two divariant, single phase points (one of which is *Diopside* in this case), the system must at some moment consist of the two end-point phases. At that time the system loses a degree of freedom and becomes univariant, and at a given P and T is therefore constrained to lie somewhere along a univariant path (in this case, a path of decreasing μ_{CaO} and increasing μ_{SiO_2}). To understand the first point, we must realize that for an *n*-component system in which $m < n - 1$ components are varying independently, (*n-m*-1)-phase regions will be separated by (*n-m*)-phase regions. In Step 2 at East Ridge, the system is merely approximated by SiO_2-$AlO_{3/2}$-MgO-CaO and Figure 5 is therefore merely a projection of the (*n-m*-1)- and (*n-m*)-phase regions onto the three-

TABLE 6. Step 2 Volume Changes and Net Relative Movement of Components

$AlO_{3/2}$ frame;	$AlO_{3/2}$ frame;	MgO frame;
dr zone	DIOP zone	DIOP zone
59.67% of original volume of qtz. monz.	11.11% of original volume of marble	74.90% of original volume of marble
Addition of components:	Addition of components:	Addition of components:
SiO_2 -3.149 moles/100 cm^3	SiO_2 -1.661 moles/100 cm^3	SiO_2 +1.986 moles/100 cm^3
CaO + .483	CaO -14.76	$\frac{1}{2}Al_2O_3$ +.100
MgO - .040	MgO -7.85	CaO -.919
FeO - .062	FeO -.065	FeO
$\frac{1}{2}Na_2O$ + .136	$\frac{1}{2}Na_2O$ -.746	$\frac{1}{2}Na_2O$

(+) = into zone
(-) = out of zone

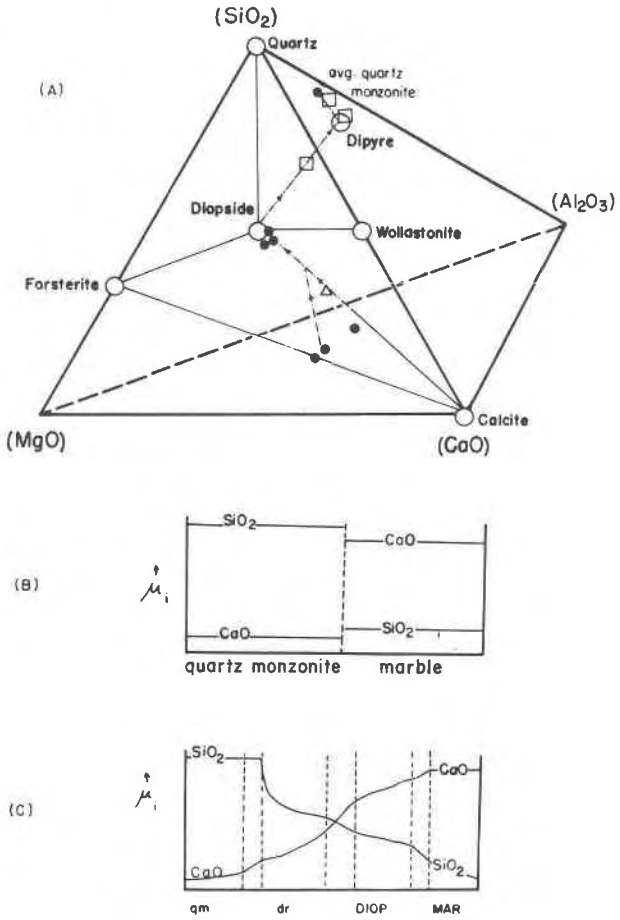

FIG. 5. a. Plot of pre-Fe-diopside Step 2 compositional variation. Dash-dot line is possible complete variation. ●, analyzed samples; □, observed at Area 1; △, observed at East Ridge. b. Schematic diagram of variation in μ_{SiO_2} and μ_{CaO} from quartz monzonite to marble, initially; and c. after formation of contact zones.

dimensional diagram; falling directly on any 4-component, univariant line of Figure 5 would be fortuitous.

The role that the volatile phase composition gradient plays concerns only the presence or absence of wollastonite, and is therefore minor compared to the non-volatile activity gradients. Inspection of Figure 6 shows that for the pure system at a fixed X_{CO_2}, the temperature must be increased from *A* to a temperature well above the curve Tr + Cc = Fo + Di + CO_2 + H_2O, if wollastonite is to become stabilized relative to calcite and SiO_2. At or below the temperature of the intrusion (for our purposes, a temperature on or just above the curve Tr + Cc = Fo + Di + CO_2 + H_2O), wollastonite will be stabilized by a decreased X_{CO_2} in the fluid phase (arrow, Fig. 6), as shown by Greenwood (1969). Therefore it appears that a variation in fluid composition between an H_2O-rich fluid in the magma and a CO_2-rich fluid in the marble, determined the presence or absence of wollastonite in the contact area.

Formation of Mizzonite and Fe-Diopside. It is clear that mizzonite formed after the formation of the *dr* and DIOP contact zones and the Fe-diopside by the inclusions of Fe-diopside and dipyre in the mizzonite. Whether Fe-diopside formed during or after the formation of the *dr* zone is unclear, and therefore two hypotheses for the formation of the two minerals will be discussed. Both account for the fact that the net result of this process, which mostly involved changing the *dr* into a SCAP zone, is the addition of 0.1 moles/100 cm^3 SiO_2, 0.03 moles/100 cm^3 CaO, 0.13 moles/100 cm^3 FeO, and 0.06 moles/100 cm^3 MgO, based on the $AlO_{3/2}$ reference frame.

One possibility is that the CaO, MgO, FeO, and SiO_2 rejected from the DIOP zone first formed Fe-diopside concurrently with the other Step 2 processes; these components precipitated pyroxene in the adjacent quartz monzonite as well. CaO reacted with the dipyre to form mizzonite and quartz: (roughly) $5CaNa_2Al_4Si_8O_{24}\cdot(CaCO_3)_{0.3}$ + 2CaO + 2.1 CO_2 → $4Ca_2NaAl_5Si_7O_{24}\cdot(CaCO_3)_{0.9}$ + $3Na_2O$ + $12SiO_2$. Mizzonite formed in the quartz monzonite at the expense of plagioclase in much the same way, accounting for the vein-like character of the SCAP zone (Fig. 2). This process followed the formation of Fe-diopside because SiO_2 must be diluted for (1) to proceed as written. An alternative possibility is that an Fe-Mg-Si-Ca-bearing fluid phase, perhaps released by the magma, reacted with the initial Step 2 configuration to form Fe-diopside and mizzonite.

The major drawback of the first possibility is that the two minerals are not present at Area 1; unless conditions there were considerably different from those at East Ridge, it is not obvious why Fe-diopside and mizzonite should not have formed at Area 1 under this model. This drawback does not exist for the second possibility, but another does: why is no other evidence of this fluid, such as veins containing Mg-bearing minerals, seen in the quartz monzonite?

The problem may have a solution in light of the zoned Fe-diopside/mizzonite veins of the MAR zone. The minerals of these veins are virtually identical to the Fe-diopside and mizzonite of the SCAP zone, which would suggest an identical origin. The MAR zone veins are merely quartz monzonite sills which have reacted with the marble *at constant volume of the vein,* as can be shown by a straightforward com-

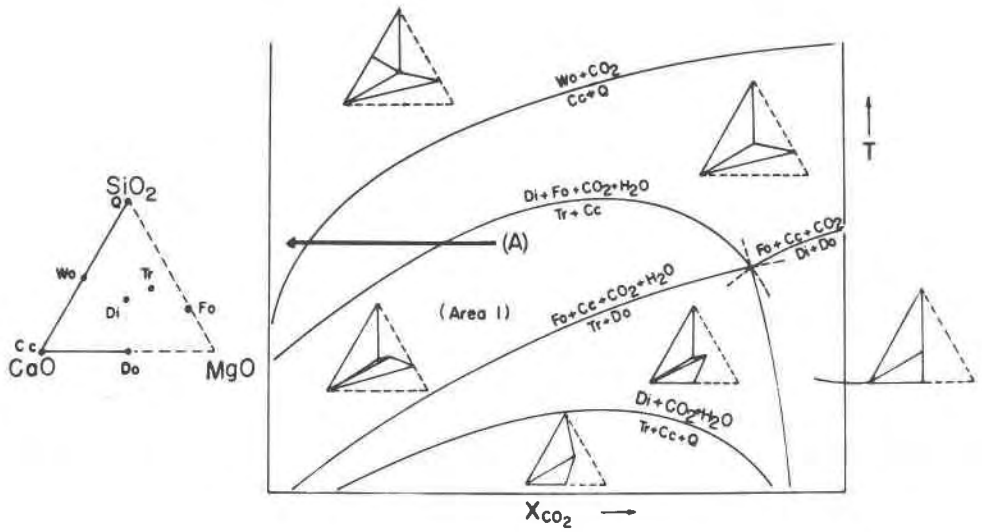

FIG. 6. Schematic T-X_{CO_2} plot of some assemblages and reactions in siliceous dolomites at ~4 kbar. Based on data from Greenwood (1967), Robie and Waldbaum (1968), Metz and Trommsdorff (1968), and Skippen (1974). "A" refers to text.

parison: the average $AlO_{3/2}$ density for the veins is 0.715 moles/100 cm³, and the average SiO_2 density is 3.052 moles/100 cm³. From Table 5, the analogous figures for quartz monzonite are 0.722 and 3.022, respectively. CaO does not match but could be accommodated by the decarbonation of a volume of MAR zone equal to 60 percent of the vein, making a total volume loss of 38 percent.

This process, operating in the MAR zone veins to form Fe-diopside and mizzonite, is probably the same process responsible for the formation of these minerals in the SCAP zone as well. The figure for total volume loss for the MAR zone veins does not match the figure calculated for the DIOP/and *dr* zones (56.5%), possibly owing to differences in contact geometry. The absence of Fe-diopside and mizzonite at Area 1 remains unexplained.

Step 3

The formation of actinolite, garnet, epidote, calcite, and quartz clearly followed Steps 1 and 2, as seen by petrographic and field relations. Likewise, these five minerals seem to have all formed at the same time and by similar processes, such that the outer part of the DIOP zone became ACT, and the inner part of the SCAP zone became EP. Based on the $AlO_{3/2}$ reference frame, a 70 percent volume increase, and the addition of 1.93 moles/100 cm³ SiO_2, 1.12 moles/100 cm³ CaO, and 0.1 moles/100 cm³ FeO and 0.243 moles/100 cm³ H_2O accompanied the transition from DIOP to ACT. A 30 percent volume increase and the addition of 1.59 moles/100 cm³ SiO_2, 0.82 moles/100 cm³ CaO, 0.32 moles/100 cm³ $FeO_{3/2}$, and 0.267 moles/100 cm³ H_2O accompanied the transition SCAP to EP. These figures, and the presence of epidote veins running from the quartz monzonite to the EP zone, suggest that the Step 3 mineralization was caused by a late stage fluid which may have been liberated from the cooling quartz monzonite. That this fluid appeared well after the initial intrusion is indicated by the presence of calcite + quartz, which requires low temperatures in the presence of a high X_{H_2O} fluid (Fig. 7; Greenwood, 1967).

The chemical potential of SiO_2 is fixed in the ACT and EP zones because quartz is present. At constant temperature, pressure, and fluid composition (which fixes μ_{CaO} as calcite is also present), the only components whose chemical potentials might provide the varying conditions necessary for the observed mineral segregations are aluminum, iron (expressed herein as $FeO_{3/2}$), and magnesium. Figure 7 is a sketch of the stability fields of the East Ridge actinolite, epidote, and garnet with respect to $\mu_{AlO_{3/2}}$, $\mu_{FeO_{3/2}}$, and μ_{MgO}, at fixed P, T, fluid composition, and CaO content of the phases. This diagram illustrates why only epidote and actinolite are present in what was originally DIOP zone (high μ_{MgO}), and why epidote predominates toward the SCAP zone (higher $\mu_{AlO_{3/2}}$). Note that the f_{O_2} may have played a role here as well; all of the iron in the epidote and

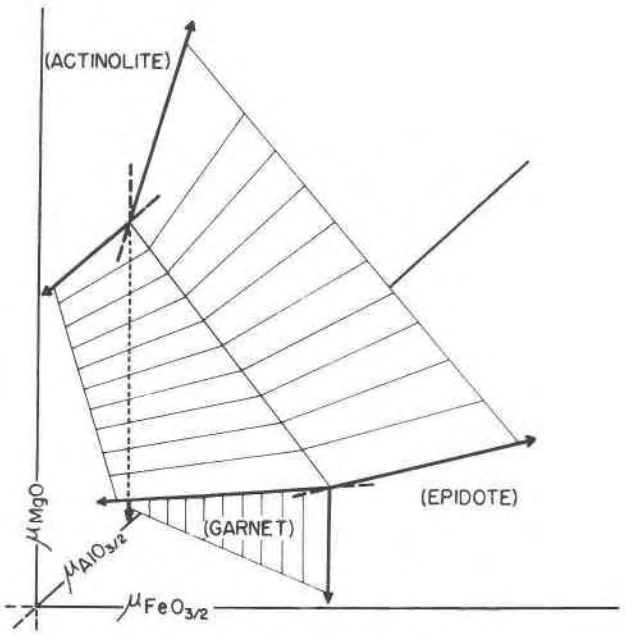

FIG. 7. Sketch of the stability fields of the East Ridge actinolite, garnet, and epidote, as they vary with μ_{MgO}, $\mu_{AlO_{3/2}}$, and $\mu_{FeO_{3/2}}$, at fixed P, T, fluid composition, and CaO content.

garnet is ferrous, whereas only 68 percent of the iron in the actinolite is in the reduced +2 state.

In the inner SCAP zone, μ_{MgO} is low, and epidote and garnet are stable relative to actinolite. The differences in stability conditions between epidote and garnet are more clearly shown by Gordon and Greenwood's (1971) work on the pure aluminum end members, zoisite and grossularite. This work established both grossularite's instability relative to zoisite at high X_{CO_2} of the fluid phase, and the wide stability range of zoisite. Assuming that these relations hold qualitatively for the iron-bearing system, the EPE subzones may represent pockets of high X_{CO_2} fluid and the EPG, pockets of low X_{CO_2} fluid or, from Figure 6, low $\mu_{AlO_{3/2}}$. Either condition could result from local concentrations of dipyre inclusions (see (1)). The southward-increasing epidote:garnet ratio observed at East Ridge may be correlative with the decreasing degree of pervasive intrusion in the same direction, for the fluid phase was probably richer in CO_2 going south, favoring epidote.

A question which remains is: why have epidote and garnet not replaced all of the SCAP zone, and actinolite, all of the DIOP? Various features indicate that the cause is not chemical in nature: epidote is apparently stable under the conditions of the SCAP zone, judging by the thin epidote veins; the EP zone occurs as small pods in the SCAP zone, apart from the regular, concentric zonation; and veins of epidote are present throughout the surrounding quartzite, schist, and gneiss. These features suggest that infiltration metasomatism, and therefore permeability, played a key role in the Step 3 process, as then mineralization would only occur where the rock was sufficiently permeable to allow reactive fluids to flow through it. If this was so, then the permeability was evidently greatest on either side of the *dr*/DIOP contact zone, dropping off rapidly with distance.

Conclusions

Three steps were involved in the formation of the East Ridge skarns. The first involved the formation of tremolite and forsterite at the expense of dolomite, calcite, and quartz, which occurred during regional metamorphism.

The second and third steps can be chronicled using a fixed-component reference frame. The second step began with the intrusion of the Cactus Quartz Monzonite, which raised the temperature of the marble, stabilizing the assemblage diopside + forsterite. At the quartz monzonite-marble contact, a zone of diopside and a zone of dipyre (sodic scapolite) began to form about the contact, due to the diffusion of Ca, Mg, and Si. Wollastonite became stable relative to calcite + SiO_2 near the marble, due to a high X_{H_2O} fluid phase. The components expelled from the contact zone formed Fe-diopside and reacted with the dipyre to form mizzonite (calcic scapolite) and quartz. The Step 2 process involved a 56.5 percent volume loss.

In the third step, mizzonite of the inner SCAP zone and Mg-diopside of the outer DIOP zone reacted with a late-stage fluid liberated from the quartz monzonite, forming epidote, garnet, and actinolite where infiltration of the fluid was possible.

Acknowledgments

This paper is a summary and extension of an undergraduate thesis submitted to U.C.L.A. in June, 1974. I am grateful to W. G. Ernst and Douglas Rumble III for their assistance and direction, and I am particularly indebted to John B. Brady for the exceedingly generous amount of time he spent on my behalf. I thank W. G. Ernst, D. Rumble III, T. M. Gordon, D. A. Hewitt, and J. B. Brady for their comments on preliminary drafts, and I owe especial thanks to an isolated system whose components' nonideal behavior increased my activity. This work was supported by a U.C.L.A. Undergraduate Fellowship, U.C.L.A. departmental funds, and an NSF Graduate Fellowship.

References

ALLEN, C. R. (1957) San Andreas fault zone in San Gorgonio Pass, southern California. *Geol. Soc. Am. Bull.* **68**, 315-350.

ALBEE, A. L., AND L. RAY (1970) Correction factors for electron

probe microanalysis of silicates, oxides, carbonates, phosphates, and sulphides. *Anal. Chem.* **42,** 1408–1414.

ARMSTRONG, R. L., AND J. SUPPE (1973) K-Ar geochronology of Mesozoic igneous rocks in Nevada, Utah, and southern California. *Geol. Soc. Am. Bull.* **84,** 1375–1392.

BAIRD, A. K., D. M. MORTON, K. W. BAIRD, AND A. O. WOODFORD (1974) Transverse ranges province: A unique structural-petrochemical belt across the San Andreas fault system. *Geol. Soc. Am. Bull.* **85,** 163–174.

BENCE, A. E., AND A. L. ALBEE (1968) Empirical correction factor for the electron microanalysis of silicates and oxides. *J. Geol.* **76,** 382–403.

BRADY, J. B. (1975) Reference frames and diffusion coefficients. *Am. J. Sci.* **275** (in press).

CARMICHAEL, D. M. (1969) On the mechanism of prograde metamorphic reactions in quartz-bearing rocks. *Contrib. Mineral. Petrol.* **20,** 244–267.

DIBBLEE, T. W. (1964) Geologic map of San Gorgonio Mountain quadrangle. *U.S. Geol. Surv. Misc. Geol. Invest. Map* **I-431.**

GORDON, T. M., AND H. J. GREENWOOD (1971) Stability of grossularite in H_2O-CO_2 mixtures. *Am. Mineral.* **56,** 1674–1688.

GREENWOOD, H. J. (1967) Wollastonite: stability in H_2O-CO_2 mixtures and occurrence in a contact-metamorphic aureole near Salmo, British Columbia, Canada. *Am. Mineral.* **52,** 1669–1680.

GUILLEU, R. B. (1953) Geology of the Johnston Grade area, San Bernardino County, California. *Calif. Div. Mines Geol., Spec. Rep.* **31,** 18 p.

HEWETT, D. R., AND J. J. GLASS (1953) Two U-bearing pegmatite bodies in San Bernardino County, California. *Am. Mineral.* **38,** 1040–1050.

HEWITT, D. A. (1973) The metamorphism of micaceous limestones from south-central Connecticut. *Am. J. Sci.* **273-A,** 444-469.

HOLLENBAUGH, K. M. (1968) *Geology of a Portion of the North Flank of the San Bernardino Mountains, California.* Ph.D. dissertation, University of Idaho, 108 p.

JOESTEN, R. (1974) Local equilibrium and metasomatic growth of zoned calc-silicate nodules from a contact aureole, Christmas Mountains, Big Bend region, Texas. *Am. J. Sci.* **274,** 876–901.

KORZHINSKY, D. S. (1959) *Physico-Chemical Basis of the Analysis of the Paragenesis of Minerals.* Consultants Bureau, Inc., New York (transl. from Russian).

METZ, P., AND V. TROMMSDORFF (1968) On phase equilibria in metamorphosed siliceous dolomites. *Contrib. Mineral. Petrol.* **18,** 305–309.

ROBIE, R. A., AND D. R. WALDBAUM (1968) Thermodynamic properties of minerals and related substances at 298.15 K (25.0°C) and one atmosphere (1.013 bars) pressure and at higher temperatures. *U.S. Geol. Surv. Bull.* **1259,** 256 p.

SHAW, D. M. (1960) The geochemistry of scapolite, pt. I. *J. Petrol.* **1,** 218-260.

SILVER, L. T. (1971) Problems of crystalline rocks of the Transverse Ranges (abstr.). *Geol. Soc. Am. Abstr. program,* **3,** 193–194.

SKIPPEN, G. (1974) An experimental model for low pressure metamorphism of siliceous dolomites. *Am. J. Sci.* **274,** 487–509.

SOLODOVNIKOVA, L. L. (1957) K voprosu o genezisye skapolitov (On the genesis of scapolites). *Ucheniye Zapiski Leningrad Gos. Univ., Ser. Geol. Nauk.* **215,** 3–48.

THOMPSON, A. B. (1975) Calc-silicate diffusion zones between marble and pelitic schist. *J. Petrol.* **16** (in press).

THOMPSON, JR., J. B. (1959) Local equilibrium in metasomatic processes. In, P. H. Abelson, Ed., *Researches in Geochemistry.* J. Wiley and Sons, New York, p. 437–457.

TURNER, F. J. (1948) Mineralogical and structural evolution of the metamorphic rocks. *Geol. Soc. Am. Mem.* **30,** 342 p.

VAUGHN, F. E. (1922) Geology of the San Bernardino Mountains north of San Gorgonio Pass. *Univ. Cal. Publ. Geol. Sci.* **13,** 319–411.

VIDALE, R. J. (1969) Metasomatism in a chemical gradient and the formation of calc-silicate bands. *Am. J. Sci.* **267,** 857–874.

———, and D. A. Hewitt (1973) "Mobile" components in the formation of calc-silicate bands. *Am. Mineral.* **58,** 991–992.

Manuscript received, May 31, 1974; accepted for publication, December 3, 1974.